Vol 12 No 11, November 2003
1009-1963/2003/12(11)/1283-08

Chinese Physics

© 2003 Chin. Phys. Soc.
and IOP Publishing Ltd

First-order Fréedericksz transition at the threshold point for weak anchoring nematic liquid crystal cell under external electric and magnetic fields

Guan Rong-Hua(关荣华)[a)b)†] and Yang Guo-Chen(杨国琛)[b)]

[a)] *Department of Applied Physics, North China Electric Power University, Baoding* 071003, *China*

[b)] *Institute of Material Physics, Hebei University of Technology, Tianjin* 300130, *China*

(Received 20 June 2003; revised manuscript received 18 August 2003)

Based on the modified formula of Rapini-Papoular, the equilibrium equation and boundary condition of the director have been obtained and the behaviour of the Fréedericksz transition at the threshold point has been studied for weak-anchoring nematic liquid crystal cells under external electric and magnetic fields with the methods of analytical derivation and numerical calculation. The results show that, except for the usual second-order transition, the first-order Fréedericksz transition can also be induced by a suitable surface anchoring technique for the liquid crystal cell given in the paper. The conditions for the existence of the first-order Fréedericksz transition are obtained. They are related to the material elastic coefficient k_{11}, k_{33} the thickness of the liquid crystal cell, the external electric field and the strength of surface anchoring, etc.

Keywords: weak anchoring, threshold point, first-order Fréedericksz transition, electric and magnetic fields

PACC: 6130, 6470M

1. Introduction

As the alignment and Fréedericksz transition of liquid crystal (LC) molecules have a great influence on LC displays, this has been widely studied by many scientists.[1−11] The Fréedericksz transition has been thought to be second order for a long time,[12,13] but in recent years, the first-order Fréedericksz transition has been studied experimentally for a strong anchoring nematic liquid crystal (NLC) cell under external electric and magnetic fields which are perpendicular to each other.[14,15] Meanwhile, the theoretical analysis for the condition of the first-order transition has been made and the existence of a bistable state has been predicted.[16] The LC cells under external electric and magnetic fields have aroused considerable attention from researchers. On the other hand, the rapid development of anchoring technology makes the exploitation and application of the weak-anchoring LC devices a topic of particular interest. Dozov and Martinot-Lagarde[17] presented experimental evidence for the first-order Fréedericksz transition in the case of tilted weak anchoring of the LC material 5CB (4-cyano-4'-*n*-pentylbiphenyl) on substrates evaporated by means of SiO. References [18] and [19] discussed the transition problem of weak-anchoring NLC cells under a single magnetic field theoretically and drew conclusions that after the anchoring energy expressed in a first-order modified formula of Rapini-Papoular (RP), the first-order Fréedericksz transition can be found both at the threshold point and the saturation point under the creation condition.

For the two situations above, we discuss the threshold behaviour of a weak-anchoring NLC cell under external electric and magnetic fields which are perpendicular to each other. The results show that, in the cell we studied, the first-order transition can be induced by a suitable surface weak anchoring technique. The conditions for the existence of the first-order transition are also given in this paper. All the studies in this paper will provide a theoretical basis for the exploitation and application of the LC display.

†E-mail: ronghua_guan@sohu.com

2. The LC cell under external electric and magnetic fields

As in Fig. 1, we consider a weak-anchoring NLC cell of thickness l. A voltage V is applied to the LC medium by putting electrically conducting glass plates at both ends of the cell, and an external magnetic field $\boldsymbol{B}$ is also applied to the LC medium. Both the glass plates and the external magnetic field $\boldsymbol{B}$ are perpendicular to the substrates of the cell. Assuming that the distance between the electrodes is d, and the easy direction $\boldsymbol{e}$ in both substrates is the same and parallel to the substrates, we establish the Cartesian coordinate system with oz axis perpendicular to the two substrates lying at $z = 0$ and $z = l$, respectively. The easy direction $\boldsymbol{e}$ is along ox axis. Obviously, the external electric field is parallel to the initial alignment of the molecules and makes the alignment more stable. The external magnetic field is perpendicular to the initial alignment of the molecules and drives the director to rotate to the oz axis which has the same direction as the field. θ is the tilt angle of the director and is a function of z.

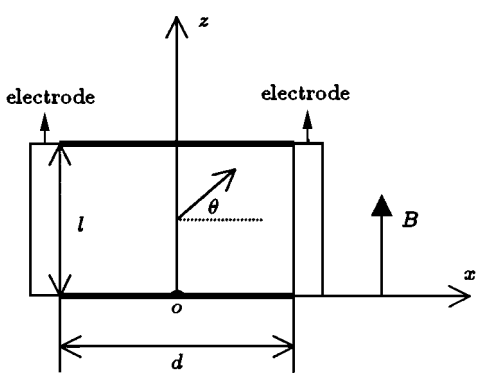


Fig.1. The model of the liquid crystal cell in external electric and magnetic fields.

The Gibbs free energy of the system consists of the following parts:

(A) The Frank's bulk density of elastic free energy

$$\begin{aligned} f_{\rm elas} =& \frac{1}{2}k_{11}(\nabla\cdot\boldsymbol{n})^2 + \frac{1}{2}k_{22}(\boldsymbol{n}\cdot\nabla\times\boldsymbol{n})^2 \\ &+ \frac{1}{2}k_{33}(\boldsymbol{n}\times\nabla\times\boldsymbol{n})^2 \\ =& \frac{1}{2}(k_{11}\cos^2\theta + k_{33}\sin^2\theta)\cdot\left(\frac{{\rm d}\theta}{{\rm d}z}\right)^2, \end{aligned} \tag{1}$$

where k_{11}, k_{33} are the Frank splay and bend elastic constants, respectively.

(B) The bulk density of the free energy of the external magnetic field

$$g_{\rm m} = -\frac{1}{2}\chi_a(\boldsymbol{H}\cdot\boldsymbol{n})^2 = -\frac{1}{2}\chi_a\frac{B^2}{\mu_0}\sin^2\theta, \tag{2}$$

where χ_a is the magnetic anisotropy of the NLC medium.

(C) The bulk density of the dielectric free energy

$$f_{\rm elec} = -\frac{1}{2}\boldsymbol{D}\cdot\boldsymbol{E} = -\frac{1}{2}\frac{\varepsilon_0\varepsilon_\parallel V^2}{d^2}\frac{1}{1+\omega\sin^2\theta}, \tag{3}$$

where $\omega = \dfrac{\varepsilon_\parallel - \varepsilon_\perp}{\varepsilon_\perp} = \dfrac{\Delta\varepsilon}{\varepsilon_\perp}$, $\varepsilon_\parallel$ and $\varepsilon_\perp$ are the principal values of the dielectric tensor, which are parallel and perpendicular to the director respectively. ε_0 is the dielectric constant of the vacuum.

(D) The surface density of anchoring free energy

The first-order modified RP formula is adopted in the surface anchoring energy, as in Refs. [18] and [19]. Then,

$$g_{\rm s}\Big|_{z=l} = \frac{1}{2}A\sin^2\theta_l(1+\zeta\sin^2\theta_l), \quad \text{for } z = l, \tag{4}$$

$$g_{\rm s}\Big|_{z=0} = \frac{1}{2}A\sin^2\theta_0(1+\zeta\sin^2\theta_0), \quad \text{for } z = 0, \tag{5}$$

where θ_0 and θ_l are the values of θ at the two substrates $z = 0$ and $z = l$ respectively. Based on the symmetry of the system, we have $\theta_0 = \theta_l$.

With Eqs. (1)–(5), the total energy of the system can be written as

$$\begin{aligned} G =& S\int_0^l \left[\frac{1}{2}(k_{11}\cos^2\theta + k_{33}\sin^2\theta)\left(\frac{{\rm d}\theta}{{\rm d}z}\right)^2\right. \\ &\left. - \frac{1}{2}\frac{\chi_a B^2}{\mu_0}\sin^2\theta - \frac{1}{2}\frac{\varepsilon_0\varepsilon_\parallel V^2}{d^2}\frac{1}{1+\omega\sin^2\theta}\right]{\rm d}z \\ &+ SA\sin^2\theta_0(1+\zeta\sin^2\theta_0), \end{aligned} \tag{6}$$

where S is the area of the substrate. Because the free energy G is the minimal in the stable state of director distribution, we can obtain the equilibrium equation and boundary condition of director distribution θ from the first-order variation δG=0.[20]

The equation is

$$\begin{aligned} &\cos\theta\sin\theta(k_{33}-k_{11})\left(\frac{{\rm d}\theta}{{\rm d}z}\right)^2 \\ &- \frac{\varepsilon_0\varepsilon_\parallel V^2}{d^2}\frac{\omega\sin\theta\cos\theta}{(1+\omega\sin^2\theta)^2} \\ &+ \frac{\chi_a B^2}{\mu_0}\sin\theta\cos\theta \\ &+ (k_{11}\cos^2\theta + k_{33}\sin^2\theta)\frac{{\rm d}^2\theta}{{\rm d}z^2} = 0, \end{aligned} \tag{7}$$

and the boundary condition is

$$(k_{11}\cos^2\theta_0 + k_{33}\sin^2\theta_0)\frac{\mathrm{d}\theta}{\mathrm{d}z}\bigg|_{z=0} = A\sin\theta_0\cos\theta_0(1+2\zeta\sin^2\theta_0). \tag{8}$$

Eqs. (7) and (8) can be used to determine the distribution of the director tilt angle θ completely.

Now, let us discuss the solutions of Eq. (7) with the boundary condition (8), so as to study the variation of the liquid crystal states with increasing external magnetic field $\boldsymbol{B}$ when the external voltage V is fixed. Obviously, there are two trivial solutions

$$\theta(z) \equiv 0, \tag{9}$$

$$\theta(z) \equiv \frac{\pi}{2}. \tag{10}$$

We call them the uniform solution and saturation solution respectively, and both of them satisfy $\dfrac{\mathrm{d}\theta}{\mathrm{d}z} = 0$. In addition, there is also the third non-trivial solution, which is called the disturbed solution. The third solution satisfies $\dfrac{\mathrm{d}\theta}{\mathrm{d}z} \neq 0$.

In order to find out disturbed solution, Eqs. (7) and (8) are transformed as follows:
From Eq. (7), we obtain

$$\frac{\mathrm{d}}{\mathrm{d}z}\left[(k_{11}\cos^2\theta_0 + k_{33}\sin^2\theta_0)\left(\frac{\mathrm{d}\theta}{\mathrm{d}z}\right)^2 + \frac{\varepsilon_0\varepsilon_\parallel V^2}{d^2}\frac{1}{1+\omega\sin^2\theta} + \frac{\chi_a B^2}{\mu_0\sin^2\theta}\right] = 0, \tag{11}$$

that is,

$$\frac{\mathrm{d}\theta}{\mathrm{d}z} = \sqrt{\frac{c(\theta_\mathrm{m}) - c(\theta)}{k_{11}(1+\gamma\sin^2\theta)}}, \quad \left(0 \le z \le \frac{l}{2}\right), \tag{12}$$

where $\gamma = \dfrac{k_{33}-k_{11}}{k_{11}}$. θ_m is the tilt angle of the director $\boldsymbol{n}$ at the middle layer $z = l/2$. From the symmetry of the surface anchoring at the top and bottom substrates, we know that θ reaches maximum at $z = l/2$ and satisfies $\dfrac{\mathrm{d}\theta}{\mathrm{d}z}\bigg|_{z=\frac{l}{2}} = 0$. $c(\theta)$ is a term related to θ, and expressed as

$$c(\theta) = \frac{\varepsilon_0\varepsilon_\parallel V^2}{d^2}\frac{1}{1+\omega\sin^2\theta} + \frac{\chi_a}{\mu_0}B^2\sin^2\theta. \tag{13}$$

So, Eq. (12) is the differential equation of the disturbed solution θ, which is derived from Eq. (7). It reflects the rate of the spatial change of the director distribution in the disturbed state. Equation (12) can be further transformed into an integral equation

$$\int_{\theta_0}^{\theta_\mathrm{m}} \sqrt{\frac{c(\theta_\mathrm{m}) - c(\theta)}{k_{11}(1+\gamma\sin^2\theta)}}\,\mathrm{d}\theta = \frac{l}{2}. \tag{14}$$

The boundary condition (8) can be re-expressed, by using Eq. (14), as

$$\sqrt{k_{11}(1+\gamma\sin^2\theta)}\sqrt{c(\theta_\mathrm{m}) - c(\theta)} = A\sin\theta_0\cos\theta_0(1+2\zeta\sin^2\theta_0). \tag{15}$$

We have obtained the equilibrium Eqs. (12) and (14) (one is a differential equation, the other is an integral equation) and surface condition (15), which the disturbed solution satisfies. With the three equations, the director distribution in the disturbed state can be solved.

We can see that equilibrium state Eq. (7) with the boundary condition (8) has three solutions. The uniform solution (9) corresponds to the state in which the director keeps the initial undisturbed spatial distribution. The saturation solution (10) corresponds to the state in which the director aligns along the external field completely. The solution satisfying Eqs. (8) and (9) corresponds to the disturbed distribution of director. When the external field is given, the alignment of the molecules depends on which solution makes the free energy minimal.

Denoting the three solutions above by G_0, G_S and G_θ respectively, Eq. (6) yields

$$G_0 = Sl\left[-\frac{1}{2}\frac{\varepsilon_0\varepsilon_\parallel V^2}{d^2}\right], \tag{16}$$

$$G_S = Sl\left[-\frac{1}{2}\frac{\varepsilon_0\varepsilon_\parallel V^2}{d^2}\frac{1}{1+\omega} - \frac{1}{2}\frac{\chi_a}{\mu_0}B^2\right] + SA(1+\zeta), \tag{17}$$

$$G_\theta = S\left\{\int_0^l [c(\theta_\mathrm{m} - c(\theta)]dz - \frac{1}{2}c(\theta_\mathrm{m})l\right\} + SA\sin^2\theta_0(1+\zeta\sin^2\theta_0). \tag{18}$$

Generally, When the external magnetic field begins to increase from zero, the value of G_0 will be the first becoming the smallest, and solution (9) is the most stable. Then when the external field $\boldsymbol{B}$ increases to some value denoted by B_th, G_θ will become the smallest, and the director distribution begins to change and the disturbed solution (12) is the most stable. B_th is the so-called threshold field. When $\boldsymbol{B}$ increases to another special value denoted by B_sat, G_S becomes the smallest, and the director distribution will change again and reach a saturation state (10) finally. B_sat is the so-called saturation field. We can see that B_th is determined by $G_\theta = G_0$.

In order to study the threshold behaviour of the weak anchoring NLC cell under electric and magnetic fields, we introduce a new parameter and a new variable denoted by u and v respectively.

$$u = \sin^2 \theta_{\rm m}, \tag{19}$$

$$v = \frac{\tan^2 \theta}{\tan^2 \theta_{\rm m}}. \tag{20}$$

For the uniform solution (9), u=0; for the saturation solution (10), u=1; and for the disturbed solution, $0 < u < 1$. Here, u is equivalent to the order parameter in Landau-de Gennes theory, which has been used in Ref. [16]. Now the reduced anchoring strength α, reduced free energy density g_θ and reduced magnetic field b are also introduced

$$\alpha = \frac{Al}{2k_{11}}, \tag{21}$$

$$g_\theta = \frac{2Sk_{11}}{l}, \tag{22}$$

$$b = \frac{B}{B_{\rm c}^0}. \tag{23}$$

Where $B_{\rm c}^0 = \dfrac{\pi}{l}\sqrt{\dfrac{\mu_0 k_{11}}{\chi_a}}$ is the threshold magnetic field under strong anchoring. From the above equations and using Eq. (13), through a complex transformation, the integral Eq. (14), boundary condition (15) and the corresponding free energy (18) of the disturbed solution can be re-expressed, using u, as

$$b = \frac{2}{\pi} I_1, \tag{24}$$

$$I_1 = \alpha\sqrt{p}\left\{1 + \frac{1}{4\alpha^2}\left(\frac{l}{d}\right)^2 \frac{q}{p}\right\}^{1/2}, \tag{25}$$

$$\begin{aligned} g_\theta =& \frac{e}{4\omega}\left[\frac{1}{1+\omega u} - \frac{2I_3}{I_1}\right] + u(I_1^2 - 2I_1 I_2) \\ &+ \frac{\alpha u v_0}{1-u+uv_0}\left(1 + \frac{\zeta u v_0}{1-u+uv_0}\right), \end{aligned} \tag{26}$$

where

$$p = \frac{v_0}{1-v_0}\frac{1}{1-u+uv_0(1+\gamma)}\left(1 + \frac{2\zeta u v_0}{1-u+uv_0}\right)^2, \tag{27}$$

$$q = \frac{e}{(1/d)^2}\frac{1-u+uv_0}{(1+\omega u)[1-u+uv_0(1+\omega)]}, \tag{28}$$

$$e = \frac{\varepsilon_0 \varepsilon_\parallel V^2 \omega}{k_{11}}\left(\frac{l}{d}\right)^2, \tag{29}$$

$$I_1 = \int_{v_0}^{1} \frac{1}{2\sqrt{v(1-v)}}\sqrt{1-u+uv(1+\gamma)}\sqrt{R} \times \frac{{\rm d}v}{1-u+uv}, \tag{30}$$

$$I_2 = \int_{v_0}^{1} \frac{v}{2\sqrt{v(1-v)}}\sqrt{1-u+uv(1+\gamma)}\sqrt{R} \times \frac{{\rm d}v}{(1-u+uv)^2}, \tag{31}$$

$$I_3 = \int_{v_0}^{1} \frac{1}{2\sqrt{v(1-v)}}\sqrt{1-u+uv(1+\gamma)}\sqrt{R} \times \frac{{\rm d}v}{1-u+uv(1+\omega)}, \tag{32}$$

and

$$R = 1 + \frac{\left(\dfrac{l}{d}\right)^2 q \dfrac{1-u+uv_0(1+\omega)}{1-u+uv(1+\omega)}}{4\alpha^2 p + \left(\dfrac{l}{d}\right)^2 q\left(\dfrac{u(1+\omega)(v-v_0)}{1-u+uv(1+\omega)}\right)}. \tag{33}$$

Because foundation functions I_1, p, q are all functions of u and v_0, and from Eq. (25) we know that v_0 is an implicit function of u, there is only one independent variable u in the above equations. In order to discuss the threshold behaviour of LCs, the values of disturbed solution and uniform solution need to be compared. Defining the difference of the two reduced free energies by g,

$$\begin{aligned} g =& g_\theta - g_0 \\ =& \frac{e}{4\omega}\left[\frac{1}{1+\omega u} - \frac{2I_3}{I_1} + 1\right] \\ &+ u(I_1^2 - 2I_1 I_2) \\ &+ \frac{auv_0}{1-u+uv_0}\left(1 + \frac{\zeta u v_0}{1-u+uv_0}\right), \end{aligned} \tag{34}$$

using Eqs. (24), (25) and (34), we can discuss the Fréedericksz transition. For a given u, from Eqs. (24) and (25) we can solve v_0 and b, then using Eqs. (34), (30)–(32) and (27), (28), (33) we can obtain g. Denoting u at the threshold point by $u_{\rm c}$, then we obtain

$$g(u_{\rm c}) = 0, \tag{35}$$

$u_{\rm c}$ can be determined by Eq. (35). If $u_{\rm c}$=0, the transition is a second-order one. Otherwise, it is first-order.

3. The transition at the threshold point

According to the method introduced above, a numerical calculation can be made. Combining Eq. (25) with Eq. (30) yields

$$\int_{v_0}^{1} \frac{1}{2\sqrt{v(1-v)}} \sqrt{1-u+uv(1+\gamma)}\sqrt{R}\frac{\mathrm{d}v}{1-u+uv} = \alpha\sqrt{p}\left\{1+\frac{1}{4\alpha^2}\left(\frac{l}{d}\right)^2\frac{q}{p}\right\}^{1/2}, \quad (36)$$

which defines the implicit function $v_0(u)$. Substituting $v_0(u)$ into Eqs. (24) and (34) yields functions $b(u)$ and $g(u)$, respectively. The value of u_c is determined by $g(u) = 0$. The threshold field results from $b_{th} = b_c^0 b(u_c)$, and the property of Fréedericksz transition depends on whether u_c equals zero or not.

Taking the LC material of MBBA (4-methoxybenylidenez-4'-*n*-butylaniline) as an example, we have $k_{33}/k_{11} \approx 1.25$; $\varepsilon_{\parallel} = 5.54$; $\varepsilon_{\perp}$=5.70.[21] Suppose l/d=0.15, ω=0.2, e=6.0. We are studying the influence of different anchoring on the induction of Fréedericksz transition. So two sets of different anchoring parameters (a) α=4.0, $\zeta = -0.2$, (b) α=0.6, ζ=0.2 are chosen for comparison. The results are illustrated in Figs.2 and 3.

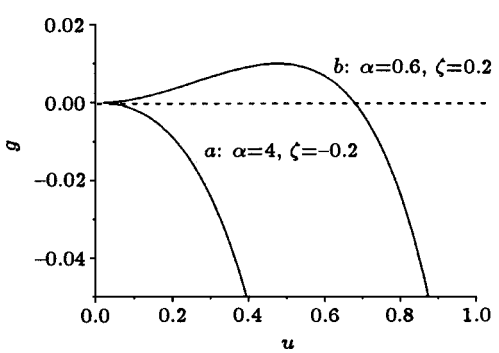


Fig.2. Variations of reduced free energy difference g with the state parameter u for γ=0.25, ω=0.2, e=6.0, l/d=0.15. The anchoring parameters are curve a: α=4.0, $\zeta = -0.2$, curve b: α=0.6, ζ=0.2.

Figure 2 shows the dependence of reduced free energy difference g of disturbed solution and uniform solution on state parameter u for different anchoring parameters curve a α=4, $\zeta = -0.2$, curve b α=0.6, ζ=0.2. Both of the curves are tangential to the horizontal axis $g(u)$=0 at u=0. For Fig. 2 curve a, the curve begins to descend at u=0. That is to say, $g \leq 0$ for $u \geq 0$ and $g(0)$=0 only for $u_c = 0$. In this case, the transition at the threshold point is a second-order one, which is usually observed. For Fig. 2 curve b, the curve rises first, then falls and intersects the horizontal axis $g(u)$=0 at u=0.680. This means that $g \leq 0$ for $u \geq 0.680$ and $u_c = 0.680$. So the transition, in this case, is a first-order Fréedericksz transition.

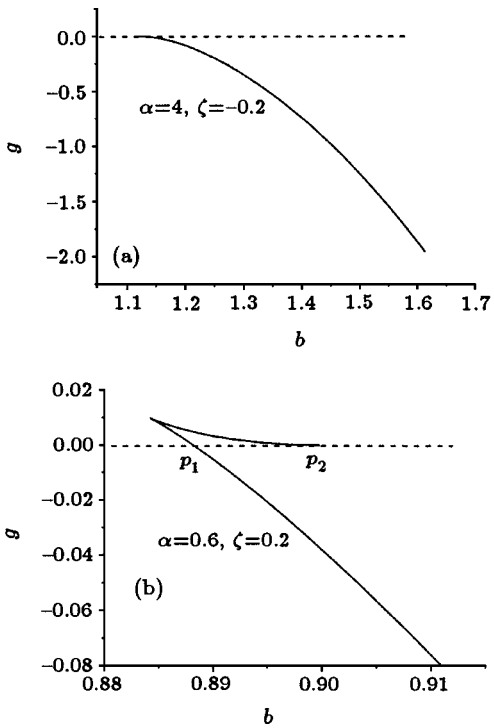


Fig.3. Variations of reduced free energy difference g with the external magnetic field b for γ=0.25, ω=0.2, e=6.0, l/d=0.15. The anchoring parameters are (a) α=4.0, $\zeta = -0.2$, (b) α=0.6, ζ=0.2.

Figure 3 depicts the dependence of reduced free energy difference g on the external magnetic field b, i.e. $g(b)$ which is obtained by combining $b(u)$ and $g(u)$ to eliminate u. The parameters used in Figs.3 (a) and 3 (b) are same as those in Figs.2 curve a and curve b respectively. In the case of Fig. 3 (a) with anchoring parameters α=4, $\zeta = -0.2$, denoting $b(0)$ by b_{th}^0, we can see from the figure that $b_{th}^0 = 1.121$, and when $b \geq b_{th}^0$, we have $g \leq 0$. So b_{th}^0 is just the reduced threshold magnetic field. We can prove that b_{th}^0 satisfies the following equation:

$$\frac{\sqrt{(\pi b_{th}^0)^2 - e}}{2\alpha} = \cot\frac{\sqrt{(\pi b_{th}^0)^2 - e}}{2}, \quad (37)$$

which is obtained by letting $u = u_c = 0$ in Eq. (24). Equation (37) is the calculation formula of the threshold field for a second-order transition of weak anchoring LC cell under electric and magnetic fields perpendicular to each other. In the case of Fig. 3 (b) with anchoring parameters α=0.6, $\zeta = 0.2$, the curve intersects the horizontal axis g=0 at two points p_1 and p_2,

which correspond to [b=0.888, u=0.680] and [b=0.898, u=0], respectively. For the curve beginning at p_1, we have $g \leq 0$. For the upper curve between the two points, there is $g \geq 0$. So p_1 corresponds to the threshold point and $b_{\rm th}$=0.888, and it is a first-order transition because of $u = u_{\rm c} = 0.680 \neq 0$. In the case of the first-order transition, Eq. (37) cannot be used to calculate the threshold field $b_{\rm th}$, which is determined by $g(b_{\rm th}) = 0$.

We have discussed only one example. The general condition for the first-order transition needs to be analysed.

4. The condition for the first-order transition

From the preceding numerical results, we see that under some conditions the first-order transition may occur. Here, we will determine the conditions for occurrence.

From Fig. 2 curves a and b, we know that the reduced free energy difference g is less than zero in the vicinity of u=0 for the second-order transition, but it is greater than zero for the first-order transition. According to this, the condition of the first-order transition can be obtained.

We can calculate the values of g and its first- and second-order derivatives at u=0 from Eqs. (24)–(26) and (30)–(32). The derived results are

$$g|_{u=0} = 0, \tag{38}$$

$$\left.\frac{{\rm d}g}{{\rm d}u}\right|_{u=0} = 0, \tag{39}$$

$$\begin{aligned}\left.\frac{{\rm d}^2 g}{{\rm d}u^2}\right|_{u=0} =& \left.\frac{{\rm d}I_1}{{\rm d}u}\right|_{u=0}\left[4(I_{1,0}-I_{2,0}) - e\frac{I_{2,0}}{I_{1,0}^2}\right] \\ &+ \left.\frac{{\rm d}I_2}{{\rm d}u}\right|_{u=0}\left(\frac{e}{I_{1,0}} - 4I_{1,0}\right) \\ &+ 2\alpha\left.\frac{{\rm d}v_0}{{\rm d}u}\right|_{u=0} + 2\alpha V_0[(1-V_0)+\zeta V_0] \\ &+ \frac{e\omega}{8}\left(1 - \frac{3 - V_0 - 2V_0^2}{\alpha}\right),\end{aligned} \tag{40}$$

where V_0, $I_{1,0}$, $I_{2,0}$ and $\left.\frac{{\rm d}v_0}{{\rm d}u}\right|_{u=0}$, $\left.\frac{{\rm d}I_1}{{\rm d}u}\right|_{u=0}$, $\left.\frac{{\rm d}I_2}{{\rm d}u}\right|_{u=0}$ are the values of v_0, I_1, I_2 and their first-order derivatives at u=0, respectively. They are determined by the following equations. Substituting u=0 into Eqs. (36), (30), (31) respectively, yields

$$a\sqrt{\frac{V}{1-V_0}} = \frac{\pi}{2} - \arcsin\sqrt{V_0}, \tag{41}$$

$$I_{1,0} = \alpha\sqrt{R_0}\frac{V_0}{1-V_0}, \tag{42}$$

$$I_{2,0} = \frac{1}{2}\sqrt{R_0}\sqrt{\frac{V_0}{1-V_0}}\cdot[\alpha + (1-V_0)], \tag{43}$$

where R_0 is the value of R at u=0, which can be obtained using Eq. (33),

$$R_0 = 1 + \frac{e}{4\alpha^2}\frac{1-V_0}{V_0}, \tag{44}$$

Taking the first-order derivative of u in Eqs. (25), (30) and (31) at u=0, we obtain

$$\left.\frac{{\rm d}v_0}{{\rm d}u}\right|_{u=0} = \frac{V_0[(1+\gamma) - 4\zeta + \omega(R_0-1)] + \dfrac{I_{2,0}}{I_{1,0}}[(\gamma-1) - \omega(R_0-1)]}{\dfrac{1}{V_0}\left[\dfrac{1}{\alpha} + \dfrac{1}{(1-V_0)}\right]}, \tag{45}$$

$$\begin{aligned}\left.\frac{{\rm d}I_1}{{\rm d}u}\right|_{u=0} =& \frac{1}{2}I_{1,0} - \frac{I_{1,0}}{2V_0}\cdot\left.\frac{{\rm d}v_0}{{\rm d}u}\right|_{u=0}\cdot\left[\frac{1}{\alpha} + \frac{R_0-1}{R_0}\frac{1}{1-V_0}\right] \\ &- \frac{I_{1,0}}{2}\cdot\frac{R_0-1}{R_0}[4\zeta V_0 + 1 - V_0(1+\gamma) + \omega - \omega V_0(R_0-1)] \\ &+ \frac{1}{2}I_{2,0}[(\gamma-1) - \omega(R_0-1)],\end{aligned} \tag{46}$$

$$\begin{aligned}\left.\frac{{\rm d}I_2}{{\rm d}u}\right|_{u=0} =& \frac{1}{16}I_{1,0}\left(3 + \frac{3 - V_0 - 2V_0^2}{\alpha}\right)[\gamma - 3 - \omega(R_0-1)] - \frac{1}{2}\left.\frac{{\rm d}v_0}{{\rm d}u}\right|_{u=0}\left[\frac{I_{1,0}}{\alpha} + \frac{R_0-1}{R_0V_0(1-V_0)}I_{2,0}\right] \\ &+ \frac{1}{2}I_{2,0}\left\{3 - \frac{R_0-1}{R_0}[4\zeta V_0 + 1 - V_0(1+\gamma) + \omega - \omega V_0(R_0-1)]\right\}.\end{aligned} \tag{47}$$

When $\left.\frac{{\rm d}^2 g}{{\rm d}u^2}\right|_{u=0} > 0$, the value of g is greater than zero in the vicinity of u=0. So the condition for the first-order transition is

$$\left.\frac{\mathrm{d}I_1}{\mathrm{d}u}\right|_{u=0}\left[4(I_{1,0}-I_{2,0})-e\frac{I_{2,0}}{I_{1,0}^2}\right]+\left.\frac{\mathrm{d}I_2}{\mathrm{d}u}\right|_{u=0}\left(\frac{e}{I_{1,0}}-4I_{1,0}\right)$$
$$+2\alpha\left.\frac{\mathrm{d}v_0}{\mathrm{d}u}\right|_{u=0}+2\alpha V_0[(1-V_0)+\zeta V_0]+\frac{e\omega}{8}\left(1-\frac{3-V_0-2V_0^2}{\alpha}\right)>0. \quad (48)$$

For a given LC cell, the parameters α, ζ, ω, e are known, and we can judge the threshold behaviour by Eqs. (48) and (41)–(47).

In order to understand well the condition for the first-order transition, we consider α and ζ as variables, and plot the Fréedericksz phase diagram for ω=0.2, e=6.0, γ=0.25. The result is illustrated in Fig. 4.

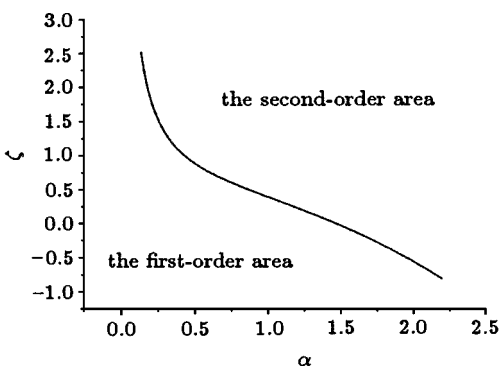


Fig.4. The Fréedericksz phase diagram for γ=0.25, ω=0.2, e=6.0, l/d=0.15, which is determined by anchoring parameters α and ζ.

In Fig. 4, the curve represents $\left.\frac{\mathrm{d}^2g}{\mathrm{d}u^2}\right|_{u=0}=0$. It divides the space into two areas, one is for the first-order transition; the other is for the second-order one. It means that, under given conditions, when the external electric and magnetic fields are together applied to the cell and the values of anchoring parameters α, ζ are taken in the second-order transition area, the second-order transition would occur at the threshold point, such as the case of taking parameter (a) in the preceding section. When the values of α, ζ are taken in the first-order transition area, the first-order Fréedericksz transition is induced by surface anchoring, such as the case of taking parameter (b) in the preceding section.

5. Conclusion

The first-order modified RP formula has been adopted to describe the surface anchoring energy. The weak anchoring NLC cell under external electric and magnetic fields, which perpendicular to each other, is investigated by strict analytic derivation and numerical calculations. The equation and boundary condition of the director in equilibrium state are obtained. The threshold behaviour has been discussed. Results obtained show that, for the investigated system, there exists the usual second-order Fréedericksz transition. But under an appropriate condition, the first-order Fréedericksz transition can occur. The condition for the first-order transition to occur is given in this paper, which is related to the material elastic coefficients k_{11}, k_{33}, the thickness of the liquid crystal cell, the external fields, and the strength of surface anchoring, etc.

At present, weak anchoring can be obtained experimentally in two ways.[22] One is by spray of SiO or other organic compound on the substrates. The other is by rubbing the surface in different degrees. Different surface treatment can provide different anchoring parameters. So, the adoption of suitable anchoring technique can induce the first-order Fréedericksz transition.

References

[1] Chen S T and Wu J J 1998 *Appl. Lett.* **52** 1988
[2] Zel'dovich B Ya, Tabiryan N V and Chilingaryan Yu S 1981 *Zh. Eksp. Teor. Fiz.* **81** 72
[3] Xv Z D *et al* 1999 *Acta Phys. Sin.* **48** 2283 (in Chinese)
[4] Durbin S D, Arakelian S M and Shen Y R 1981 *Phys. Rev. Lett.* **47** 1411
[5] Ong H L 1983 *Phys. Rev.* A **28** 2393
[6] Liang Z Y *et al* 2000 *Acta Phys. Sin.* **49** 1114 (in Chinese)
[7] Wang J and He S L 2001 *Acta Phys. Sin.* **50** 926 (in Chinese)
[8] Zhang Z D, Yu H and Li L 2001 *Chin. Phys.* **10** 645
[9] Nersisyan S R and Tabiryan N V 1984 *Mol. Cryat. Liq. Cryst.* **116** 111
[10] Ong H L 1985 *Phys. Rev.* A **31** 3450
[11] Karn A J, Arakelian S M and Shen Y R 1986 *Phys. Rev. Lett.* **57** 448
[12] Deuling H J 1972 *Mol. Cryst. Liq. Cryst.* **19** 123

[13] Gruler H, Scheffer T J and Meier G Z *Naturforsch* **27a** 966
[14] Frisken B J and Palffy-Muhoray P 1989 *Phys. Rev.* A **39** 1513
[15] Allender D W, Frisken B J and Palffy-Muhoray P 1989 *Liq. Cryst.* **5** 735
[16] Frisken B J and Palffy-Muhoray P 1989 *Phys. Rev.* A **40** 6099
[17] Dozov I and Martinot-Lagarde Ph 1998 *Phys. Rev.* E **58** 7422
[18] Yang G C, Shi J R and Liang Y 2000 *Liq. Cryst.* **3** 875
[19] Yang G C and Zhang S H 2002 *Liq. Cryst.* **29** 641
[20] Jeffreys H and Jeffreys B S 1950 *Methods of Mathematical Physics* (Cambridge: Cambridge University Press) p318
[21] Haller I 1972 *Chem. Phys.* **57** 1400
[22] Sonin A 1995 *The Surface Physics of Liquid Crystals* (New York: Gordon and Breach) p6